Exp Fluids
DOI 10.1007/s00348-010-0925-x

RESEARCH ARTICLE

Ensemble-Empirical-Mode-Decomposition method for instantaneous spatial-multi-scale decomposition of wall-pressure fluctuations under a turbulent flow

Sébastien Debert · Marc Pachebat · Vincent Valeau · Yves Gervais

Received: 9 October 2009 / Revised: 16 June 2010 / Accepted: 23 June 2010

Abstract This work illustrates the possibilities of the Ensemble-Empirical-Mode-Decomposition (E-EMD) technique for a detailed analysis of the time and space characteristics of the wall-pressure fluctuations under a turbulent flow. Pressure fluctuations are measured with a linear microphone array, for the cases of a turbulent boundary layer and for a diffuse airborne acoustic field. The E-EMD technique is shown to be an efficient tool for representing the spatial scales of the turbulent fluctuations at each instant. In particular, this representation is obtained without any particular assumption or a priori information on the data (e.g. temporal or spatial stationarity of the wall pressure data is not required), and acts, when applied to wide-band turbulent signals, as a wavenumber filter. Finally, it is shown how, to some extent, the E-EMD technique can separate at each instant the acoustic (propagative) from the hydrodynamic (convective) energy.

S. Debert · V. Valeau · Y. Gervais (✉)
UPR 3346, Département Fluides, Thermique, Combustion ESIP, Institut P', CNRS, Université de Poitiers, ENSMA, Bâtiment B17, BP633 - 6 rue Marcel Doré, 86022 Poitiers, France
e-mail: vincent.valeau@lea.univ-poitiers.fr

M. Pachebat
PSA-Peugeot-Citroën R&D, 78943 Vélizy-Villacoublay Cedex, France

Present Address:
M. Pachebat (✉)
SAI-Acoustique Indutrielle, 1 rue du saule trapu, BP236, 91882 Massy Cedex, France
e-mail: marc.pachebat@sai-acoustique.fr

1 Introduction

Aerodynamically induced noise within cabins of transportation vehicles is of major interest, due to the improvement towards reduction of other noise sources like engines and equipments. In particular, there is a recurrent need for methods allowing the separation of hydrodynamic convected fluctuations and acoustic propagated fluctuations. This leads the noise control engineers to search for tools that give a deeper insight into the production of sound by turbulence, excitation of solid structures by acoustic and convected wall-pressure fluctuations, before their transmission into the cabin. In particular, the knowledge of space-time characteristics of wall-pressure fluctuations is crucial for the radiation efficiency of sound by solid structures, since vibrating walls operate as wavenumber filters. Some advanced and promising numerical methods like Direct Noise Computation, consisting in solving the turbulent flow field and the induced acoustic field in the same computation, are currently under development (see for example Bogey and Bailly 2008; Suh et al. 2006), but are limited to academic cases as they require very high calculation capabilities. For that reason, a detailed knowledge of wall-pressure fluctuations exciting solid structures still rely on empirical models and experimental data analysis. The constant progress of hardware and software standards for multi-channel synchronous measurements also reinforces the need for accurate post-processing methods.

Classical post-processing methods of wall-pressure fluctuations data are usually based on wavenumber-frequency representations (see for example, Panton and Robert 1994; Lee and Sung 2001; Arguillat et al. 2005). However these methods suffer from the underlying assumption of time and spatial stationarity, making difficult the analysis of non-stationary and non-homogeneous flows. The present paper then proposes to apply a recently developed technique to the analysis of wall-pressure data. The Ensemble-Empirical-Mode-Decomposition (E-EMD) technique was proposed by Wu and Huang (2009) and is a particular way of using the Empirical Mode Decomposition (EMD), first introduced by Huang et al. (1998). The EMD technique was initially developed to give a time-frequency representation of a given time signal $x(t)$. It consists of splitting $x(t)$ into a finite number of particular signals [called Intrinsic Mode Functions (IMF)] for which one is able to define an instantaneous frequency. The key features of the EMD technique with respect to other well-established time-frequency representations (like wavelets, short-term Fourier transform, Wigner–Ville distributions, etc.) are the following : (a) the EMD is a non linear iterative algorithm, (b) it has no analytic definition, (c) the decomposition is fully data-driven and (d) is not unique. Examples of useful applications of the EMD technique on time signals are now so numerous that an exhaustive review is far beyond the scope of the present work, and a good introduction can be found in Huang and Shen (2005). Moreover, an application of EMD has been recently proposed by Huang et al. (2008) for a detailed study of the statistical properties of homogeneous turbulence time series. The present paper is an illustration of the possibilities of the E-EMD in analysing wall-pressure fluctuations under a turbulent boundary layer: in particular the E-EMD will offer the possibility to follow the time evolution of different ranges of spatial events of the wall-pressure field.

An important difference of the present study with former applications of the EMD technique is that, in order to follow the time evolution of the different spatial scales present in the space-time data, the EMD analysis is applied in the spatial dimension and at each time step, instead of being computed in the time domain. The EMD technique is then used in the spatial dimension to separate the events occurring at different spatial scales. Due to the capacity of the EMD technique for analysing non-stationary data, the proposed method can then be applied to non-homogeneous (i.e., spatially non-stationary) pressure fields. In the same way, non-stationary data (i.e., temporally non-stationary), such as intermittent phenomena, can also be analysed with the proposed method, as no particular treatment is carried out in the time dimension: the EMD technique is carried out in the spatial dimension for each time step, and in this sense, can be considered as an "instantaneous" decomposition. However, as the decomposition is carried out in the spatial dimension, the analysis is limited to a number of points equal to the number of probes in the measurement set-up (here, 64). Consequently, the number of obtained modes is weak (6) compared to the number of modes obtained in typical applications carried out in the time domain.

After a presentation of the wind-tunnel flow and measurement set-up, a detailed description of the E-EMD technique is proposed, together with a short presentation of the classical Spatial Correlogram method, used for estimating wavenumber-frequency spectra. The post-processing of the wall-pressure data is then presented with both methods, showing in particular the capabilities of the proposed E-EMD method to separate non-stationary events at different instants and for different scales. The turbulence-induced data are then mixed artificially with experimental acoustic fluctuations, in order to show that, to some extent, the proposed decomposition can separate at each instant, hydrodynamic (convective) from acoustic (propagative) fluctuations on the basis of their intrinsic spatial scales.

2 Experimental set-up

2.1 EOLE: anechoic Eiffel-type wind-tunnel

Experiments were carried out in the anechoic wind-tunnel (EOLE) of the Laboratoire d'Etudes Aérodynamiques (Poitiers, France). The measurement area is open and located in a $(4 \times 3 \times 3)$ m^3 anechoic chamber. The grazing flow enters the anechoic chamber through a (40×40) cm^2 convergent nozzle and is sucked through a (1×1) m^2 collector. An instrumented flat plate is located under the flow in the open part of the wind tunnel to generate a Turbulent Boundary Layer (TBL, Fig. 1). Flow velocity U_∞ ranges from 10 to 60 m s^{-1}. Results are presented for $U_\infty = 40$ m s^{-1}.

2.2 Remote microphone probes, acquisition system

For wall-pressure fluctuations measurements, the sensor can be flush-mounted or located behind a pinhole. The first mounting induces some spatial averaging due to the dimension of its sensitive area (Corcos 1963; Lueptow

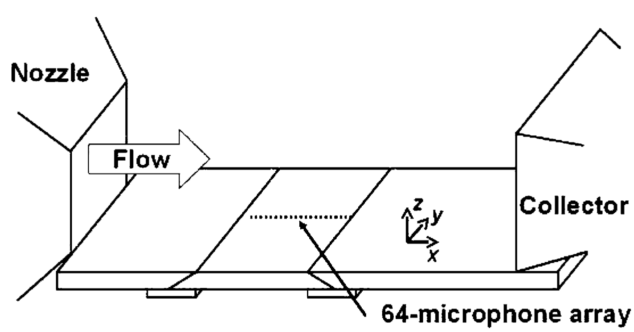

Fig. 1 Experimental set-up: the nozzle, instrumented flat plate, and collector are located in an anechoic chamber

1995). The second mounting technique, which is used here, is more appropriate, but the required spatial resolution involves the use of remote probes. To take into account the effects of the remoteness of the probes (delays, resonance modes, ...), Frequency Response Functions are used to correct the magnitude and phase of the spectra. An array of 64 remote Panasonic WM60 electret microphones is used. Small inserts (diameter of 1.3 mm) are located in the flat plate, following a streamwise line (Fig. 1). The spacing between each insert is $\Delta_x = 5.24$ mm. PVC tubes (as short as possible to reduce the low-frequency resonances) connect each insert to stainless tubes. In the middle of it, a hole (diameter of 0.5 mm) connects the tube to a small cavity where an electret microphone measures the wall-pressure fluctuations (Fig. 2). An anechoic termination of about 3 m is added to suppress the reflections produced by the end of the stainless tube. Those remote probes are connected to a 64-channels conditioning amplifier, which is then connected to a 64-channels acquisition system PAK-MKII from MÜLLER-BBM. A portion of 100 s of signal is recorded at sampling frequency $f_s = 25.6$ kHz, which gives a 10 kHz frequency band.

The calibration procedure and the calculation of the Frequency Response Functions are preliminarily carried out for each probe. A white-noise source and a reference microphone are used. As seen in Fig. 3, the source and the microphone are both connected to a very small cavity which is itself placed on the pinhole of the probe to calibrate. The cavity is designed in order to give the same pressure at the entrance of the pinhole and on the surface of the reference microphone. A 1/2″-*B&K*-4190 and a 1/4″-*B&K*-4938 microphones are respectively used as the source and the reference microphone. A portion of 40 s of signal is recorded for both the reference microphone and the probe. During the recording, the coherence between the two signals is used to validate or reject the measurement: a minimum coherence of 95% is required between 10 and

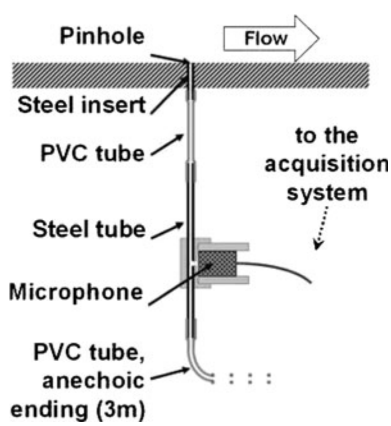

Fig. 2 Scheme of the remote microphone system for measuring wall-pressure fluctuations

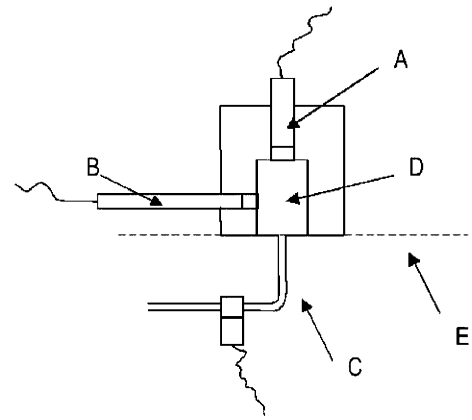

Fig. 3 Calibration system for remote probes: *A* white noise source, *B* reference microphone, *C* remote probe, *D* cavity, *E* wall

10 kHz (at least 98% between 50 and 8 kHz). The Frequency Response Functions are obtained by:

$$\mathrm{FRF}(f) = \frac{P(f).P^*_{\mathrm{ref}}(f)}{|P_{\mathrm{ref}}(f)|^2}, \tag{1}$$

where f is the frequency, $P(f)$ et $P_{\mathrm{ref}}(f)$ are, respectively, the Fourier transforms of the pressure signals of the remote probe and of the reference microphone, and where the $()^*$ symbol denotes the conjugate operator. About 50 averages of blocks of 2^{15} samples with a 33% overlap are used for the estimation of the Frequency Response Function of each sensor (Eq. 1).

2.3 LDV 2D-1 point: anemometric characterization of the Turbulent Boundary Layer

A non-invasive two-components Laser Doppler Velocimeter is used to perform anemometric measurements in the TBL. Several vertical profiles of the flow velocity were carried out in the streamwise and spanwise directions, to observe the evolution of the TBL thickness (Schlichting 1979) and to check the spanwise uniformity of the flow. The characteristics of the 40 m s^{-1}-TBL at the upstream part of the wall-pressure fluctuations measurement area are the following: TBL thickness $\delta = 18$ mm, displacement thickness $\delta_1 = 2.6$ mm, momentum thickness $\theta = 2.0$ mm, energy thickness $\delta_3 = 3.7$ mm. The first shape factor $H = \delta_1/\theta$ is about 1.3. According to Schlichting (1979), these typical values confirm that the TBL is fully developed.

2.4 Diffuse sound field recorded into a reverberation room

A reverberation room is used to create a stationary diffuse sound field which will be artificially combined to TBL-pressure data to perform tests of the separation of the acoustic and aerodynamic fluctuations (see Sect. 4.2). The volume of this room is 138 m^3 for a surface of 80 m^2. The average reverberation time is about 4 s (ranging from 8 s at 100 Hz to less than 1 s at 10 kHz). A broad-band noise is emitted using an amplifier and a speaker located in the room; 100 s of signal are recorded with a line-array of 64-microphones (spatial sampling of 6 mm). The multiple wall reflections generate acoustic waves statistically uniform in time and space, creating a diffuse sound field.

3 Post-processing: spatial correlogram and E-EMD

3.1 The classical Spatial correlogram method

In order to estimate the wavenumber–frequency spectrum $\Phi(k_x,f)$ of the wall-pressure fluctuations (where k_x is the wavenumber in the streamwise direction x), a spatial correlogram method is used (Garello 2008):

$$\Phi(k_x,f) = \int_{\infty} S_{ij}(x,f)e^{-jk_x.x}\mathrm{d}x, \qquad (2)$$

with:

$$S_{ij}(x,f) = \mathrm{E}\left[\int_{\infty} p_i(x_i,t)p_j^*(x_i+x,t+\tau)e^{-j2\pi f\tau}\mathrm{d}\tau\right], \qquad (3)$$

where E[.] is the expected value. First, the cross-power spectra $S_{ij}(x, f)$ are computed (Eq. 3) using 10 blocks of 1,024 samples (and a 33% time overlap) for the averaging process. The wavenumber–frequency spectra $\Phi(k_x,f)$ are then obtained by applying a spatial Fourier transform to the cross-power spectra $S_{ij}(x, f)$ (Eq. 2).

In this paper, the modulus $|\Phi(k_x,f)|$ of the wavenumber–frequency spectra are represented in dB scale (ref. 2×10^{-5} Pa); the horizontal and vertical axis give, respectively, the reduced wavenumber $\tilde{k} = k/2\pi$ in [m^{-1}] and frequency f in (kHz). With these units and referring to the dispersion relation $f = v \cdot \tilde{k}$, the signature in the wavenumber–frequency plane of some pressure perturbations, propagated or convected with a phase velocity v, should be a straight line with a slope equal to v, making possible the estimation of v. As an averaging process using time blocks is performed, and a Fourier transform is carried out in the spatial dimension (Eq. 3), the correlogram method requires both hypothesis of time stationarity and spatial homogeneity. The representation is used in Sect. 4 to identify in a classical manner the location of acoustic and aerodynamic energies in the wavenumber–frequency plane for the original signal $p(x, t)$, and for the different modes IMF(x, t) given by the E-EMD technique.

3.2 Ensemble empirical mode decomposition

Spatial decompositions of pressure fluctuations are carried out by using the E-EMD technique, derived from the EMD method introduced by Huang et al. (1998). The EMD is an algorithm which aims at splitting a given time signal $x(t)$ into particular zero-mean signals IMF(t) called IMF plus a trend, which sum gives exactly $x(t)$. These IMF are constructed to have an amplitude-modulation versus frequency-modulation lying in separated frequency bands, thus allowing in a second step a non-ambiguous definition of their instantaneous frequency (for example using the Hilbert transform). This leads to a time-frequency representation of $x(t)$ named Hilbert–Huang Transform. The main drawback is that there is no analytic definition of the decomposition process but the main advantage is that no assumptions are needed: the algorithm is fully data-driven, avoiding the knowledge of any a priori information on the signal $x(t)$. In particular, Huang et al. (1998) show a comparison between the EMD technique and other methods like spectrogram, wavelet analysis, Wigner–Ville distribution, evolutionary spectrum, or empirical orthogonal functions, showing clearly its practical interest for non-stationary data processing. Let us now give a short description of the EMD algorithm. For further details the reader can refer to Huang et al. (1998), Huang and Shen (2005), and Flandrin et al. (2004).

3.2.1 The EMD method

For a given time signal $x(t)$, the EMD technique considers that locally, a signal is made of fast oscillations superimposed to slow oscillations. For a local oscillation (defined, e.g. as a signal portion between two consecutive local minima), the EMD is designed to define a local "low frequency" component as the local trend $m_1(t)$, supporting a local "high frequency" component as a zero-mean oscillation or local detail $d_1(t)$, with: $x(t) = m_1(t) + d_1(t)$. By design, $d_1(t)$ is then an oscillatory signal and $m_1(t)$ oscillates slower than $d_1(t)$. If we build $d_1(t)$ to be locally zero-mean everywhere, it corresponds to what is defined to be an IMF (see Huang et al. 1998; Huang and Shen 2005). This implies that all its maxima (respectively, minima) are positive (respectively, negative). Applying recursively this decomposition to $m_i(t)$ is called the sifting process, and gives an Empirical Mode Decomposition of the original signal as follows:

$$x(t) = m_K(t) + \sum_{k=1}^{K-1} d_k(t), \qquad (4)$$

where $m_K(t)$ is the final *residue* of the decomposition, and $d_k(t)$ is called the IMF of order k. In the rest of the paper, the term IMF$_k$ denotes the function d_k.

It may be pointed out that this decomposition is not unique as the IMF depend on parameters used in the sifting algorithm, but yields in practice to IMF that are nearly perfectly orthogonal. This means in particular that at a given instant, one given frequency component of the original signal $x(t)$ is represented by one and only one IMF in the decomposition. Moreover, each decomposition gives a various number of IMF, depending on the signal $x(t)$ itself since the decomposition is data-driven. Typically, if $x(t)$ is a stationary and broad-band time signal of N_s samples, the number of IMF is approximately $K \approx \log_2(N_s)$, but K may vary significantly for any other time signal of the same length.

In the following, the EMD technique is applied to a spatial pressure signal. The decomposition is applied to $p(x, t_i)$ for a given instant t_i along the spatial dimension x, according to the spatial scales of the pressure signal. An example of such a spatial decomposition is shown in Fig. 4, in the case of pressure fluctuations under a TBL (in this particular case, K is equal to 6). As a consequence of the sifting process, for $k \approx 1$, 2, the low-order IMF $IMF_k(x, t_i)$ contain spatial variations with higher spatial frequencies, i.e., associated to higher wavenumber fluctuations. Conversely, for $k \approx K - 1$, K, the high-order IMF $\mathrm{IMF}_k(x, t_i)$ are associated with low spatial frequencies, and are then the result of low wavenumber fluctuations.

As pointed out above, the EMD will give us a varying number K of IMF for each instant t_i. This does not allow to study a given mode (or scale) as a function of time. To tackle this problem the E-EMD technique is used.

3.2.2 The Ensemble-EMD method

The E-EMD technique introduced by Wu and Huang (2009) has been tested recently for mechanical fault detection (Lei et al. 2009; Ai and Li 2008), optical fringe pattern analysis (Zhou et al. 2009) and musical tempo detection (Fulton and Soraghan 2006). It can be seen as a noise-assisted EMD: the number K of IMF (including the residue) is forced to be equal to a chosen integer K_0, by adding a broadband $n(t)$ noise to the original $x(t)$, before the decomposition. K_0 will then be of the order of $\log_2(N_s)$. The noise will be then removed by ensemble averaging over many noise trials, exactly like what is commonly achieved with noisy experimental data.

Figure 5 summarizes the principle of the proposed spatial E-EMD of wall-pressure signals. In our case, we apply the EMD method on the noisy spatial pressure signal at the instant t_i, given by $p(x, t_i) + n_j(x)$ where $n_j(x)$ is the jth noise trial. The decomposition is stored only if the number of obtained modes is equal to K_0. This process is then repeated with different white noise realizations $n_j(x)$, until a given number M of decomposition with K_0 IMF is obtained. For each IMF, the ensemble averaging of the M trials is then computed in order to remove the noise component. The effect of noise should decrease following

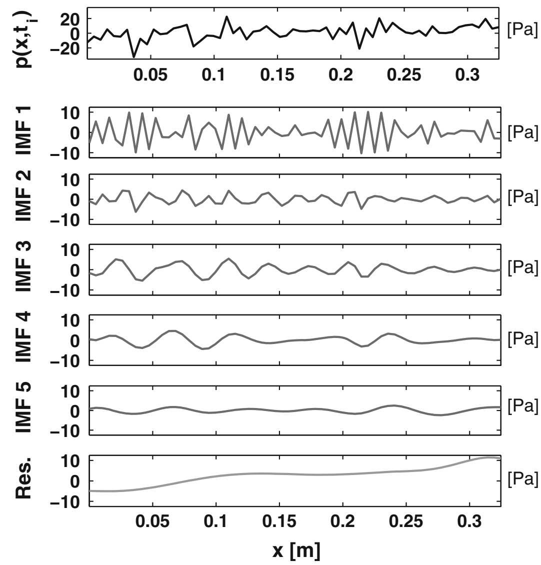

Fig. 4 Example of a decomposition of a spatial pressure signal using the EMD technique. From *top* to *bottom*: the initial pressure signal $p(x, t_i)$, the five $\mathrm{IMF}(x, t_i)$ and the residue

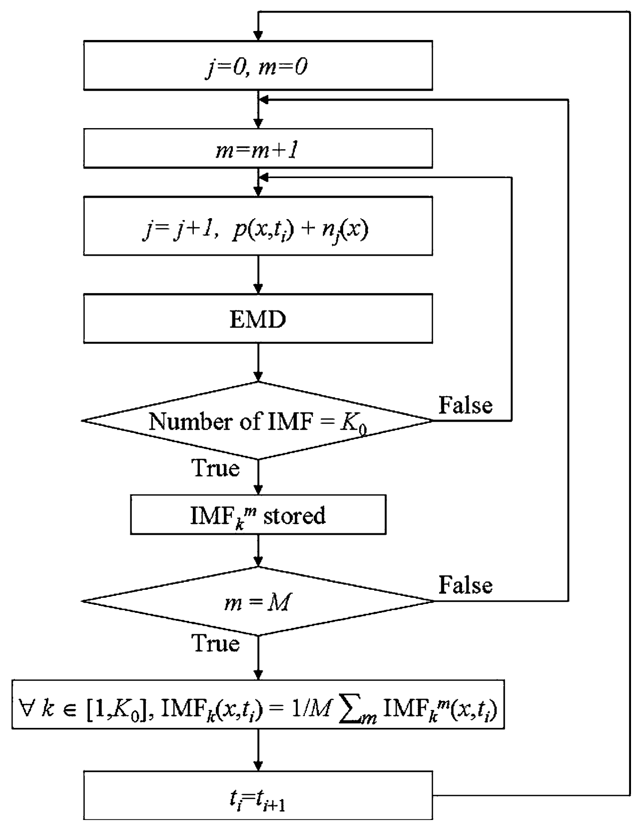

Fig. 5 E-EMD algorithm principle: from the space–time data $p(x, t)$, at each discrete instant t_i, the spatial pressure signal is extracted and decomposed into K_0 IMF (including the residue). This process is repeated for each instant t_i, and K_0 space–time data are obtained

the statistical rule (see for example Eq. (6a) in Wu and Huang 2009)

$$\varepsilon_n = \frac{\sigma(n_j(x))}{\sigma(p(x,t_i))} \cdot \frac{1}{\sqrt{M}}, \tag{5}$$

where M is the number of ensemble members, and $\sigma(s)$ denotes the standard deviation of the function s. ε_n is the error standard deviation, the error being defined as the difference between the input signal and the reconstructed signal (Eq. 4). In the following, $M = 100$ and $\varepsilon_n = 0.05$ are chosen, leading most frequently to $K = K_0 = 6$ IMF (other decompositions with $K \neq K_0$ are discarded). These parameters are similar to those used by Wu and Huang (2009) where the reader can find a detailed analysis of noise and ensemble averaging effects on decomposition. The energy of the added noise must be sufficient to force the sifting process to give the desired number of IMF K_0. On other hand, high noise level requires M to be sufficiently large to eliminate noise by ensemble averaging and have a good reconstruction of $p(x, t_i)$ (Eq. 4).

This whole process is carried out for each instant t_i of the space–time pressure data $p(x, t_i)$. Space–time pressure data are obtained for each mode of the decomposition $\mathrm{IMF}_k(x, t_i)$ and residue. This allows to study the time evolution of different ranges of spatial scales.

4 Two applications of the E-EMD technique

The E-EMD technique is now applied to two experimental configurations. Firstly, the experimental data are the measured wall-pressure fluctuations under a Turbulent Boundary Layer flow. Some observations of the space–time representation of the signals are carried out, concerning both the raw pressure-field data, and the E-EMD modes. A wavenumber–frequency analysis, based on the spatial correlogram method, is also used in order to get a further insight into the physical content of each mode. Secondly, an artificial combination of TBL wall-pressure data, and airborne diffuse sound field data is then analysed, in order to stress the interest of the E-EMD analysis for signals containing both acoustic and hydrodynamic phenomena.

4.1 Analysis of the wall-pressure fluctuations under the TBL

4.1.1 The space–time and wavenumber–frequency representations of the initial pressure signal

A space–time representation of the wall-pressure $p(x, t)$ data is shown on Fig. 6. The flow velocity is $U_\infty = 40$ m s^{-1}. The horizontal and vertical axes give,

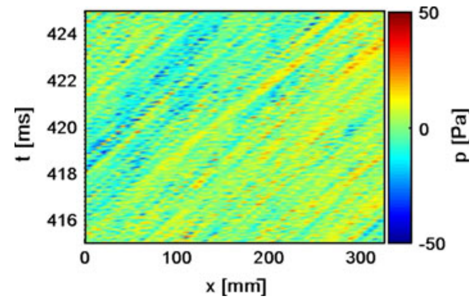

Fig. 6 Space–time representation of wall-pressure fluctuations under a 40 m s^{-1} turbulent boundary layer

respectively, the space x and time t domains in mm and ms, so that the detailed time evolution of the wall-pressure over the linear array of sensors can be observed.

The space–time representation exhibits a set of oblique patterns corresponding to the convection of pressure fluctuations along the linear microphone array. The corresponding convection velocity U_c can be estimated to be around 32 m s^{-1}, which is appreciably equal to the wall-convection velocity (about 0.8 times the flow velocity U_∞ according to Corcos 1963). One given oblique pattern is the wall signature of one given structure of the flow (an eddy), moving over the sensors array. The signature energy and broadness may vary from one to another one, according to the size and vorticity of the eddy followed by the array.

Although a general convection velocity dominates, local variations of the pattern slopes can be observed. This can have several causes: first, eddies can be convected with velocities that can differ from one to another one or they can be locally slightly convected in the spanwise direction; as a consequence the signature indicates locally a higher phase velocity. In addition, the ejection phenomena occurring in a TBL (Hinze 1975), associated to the creation of streaks and hairpins (Acarlar and Smith 1987) results in a transformation of streamwise velocity component into vertical velocity component. This can involve, in terms of wall pressure-data, a substantial decrease of the convection velocity (lower phase velocity).

The wavenumber–frequency representation is now used in order to evaluate the physical content of the pressure signal (Fig. 7a). An oblique conical signature is clearly observed: this is the signature of the aerodynamic energy of the flow, termed convective cone in the following. Using the dispersion relation, a velocity can be estimated using the main slope of the cone: about 32 m s^{-1}, which once again agrees with Corcos' relation ($0.8 \times U_\infty$). Any phenomena propagating at the velocity of sound c_0 should have a phase velocity greater than c_0. Acoustic energy should then lie within a vertical cone bounded by the $\pm c_0/2\pi$ slopes. This cone is referred to in the following as the acoustic cone.

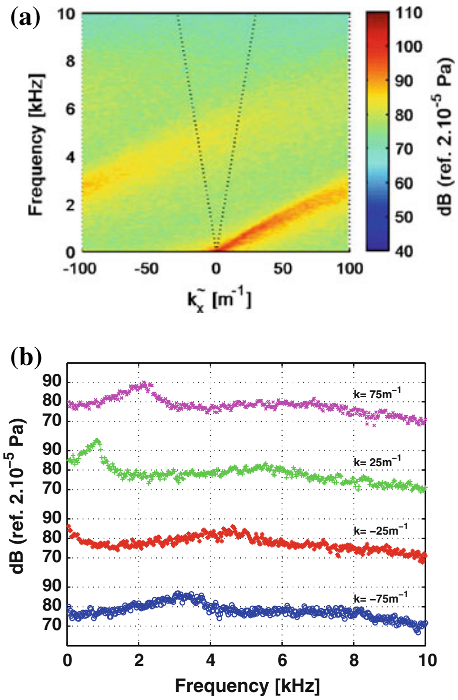

Fig. 7 Wavenumber–frequency representation (**a**) and 4 vertical sections at $k = [-75, -25, 25, 75]$ m^{-1} (**b**) of wall-pressure fluctuations under a 40 m s^{-1} turbulent boundary layer. The two *dotted lines* in **a** (indicating $\pm c_0$ phase velocities) bound the acoustic cone domain

The oblique energetic zone appearing at frequencies higher than 2 kHz is the consequence of aliasing effect, due to spatial sampling. The aliased energy is clearly observed in the vertical sections of the wavenumber-frequency representation (Fig. 7b): whereas the peaks for the sections at $k = 25$ and 75 m^{-1} account for the physical energy present in the flow, the peaks present in the sections at negative wavenumbers (about $f = 4{,}500$ and 3,500 Hz for $k = -25$ and -75 m^{-1}, respectively) contain exclusively aliased energy. Indeed, wall fluctuations with spatial scales smaller than the distance Δ_x between two sensors result in the presence of aliased convective energy in the acoustic cone. This aliasing tends to mask the acoustical energy effectively produced by turbulence and that could be detectable in the acoustic cone of the present set of data (Debert et al. 2007). Following Corcos (1963), the coefficient α_x describing stream-wise spatial coherence of the pressure field should be similar to $\alpha_x = 1/8$; thus by estimating the smallest stream–wise coherent scale with $U_c = 32$ m s^{-1}, $f_s = 25.6$ kHz, the sensor spacing should fulfil $\Delta_x \ll \frac{U_c}{\alpha_x f_s} = 0.00875\,\mathrm{m}$ to avoid the aliasing of the convective energy. This leads to a spacing of the order of 1 mm which was hardly feasible in practice.

4.1.2 E-EMD results

Using now the E-EMD technique as described in Sect. 3.2, the same TBL wall-pressure set of data is decomposed into 5 IMF and a residue.

The upper six graphs in Fig. 8a–f show the (x, t) representations of the five IMF and the residue after the application of the E-EMD algorithm on the TBL signal. In order to observe all details in each mode, the scale of each color bar in Pa is let free. This allows to observe the amplitude range of each mode: from about ±25 Pa for the first IMF to ±7 Pa for the fifth IMF. On other hand, the amplitude of the residue is greater, approximately ±15 Pa. For all IMF, oblique patterns corresponding to the same global convection of pressure fluctuations as on Fig. 6 are observed. However, the spatial scales of the convected pressure fluctuations increase with the order of the IMF. This is a consequence of the sifting process, and corroborates the example decomposition provided, for one particular instant, on Fig. 4: the first modes collect the small spatial scales, leaving the larger scales to the last modes. The decomposition indicates that small scales (low-order IMF) are more energetic than the large scales (high-order IMF). It is also noticeable that the residue, together with the IMF 5, contain an additional pattern: the same general slope as the other IMF is observed, but many nearly-horizontal streaks are visible.

The E-EMD decomposition appears to be a physically meaningful decomposition: although the decomposition is made for each instant in the spatial dimension, totally independently of the other instants, each decomposition is physically consistent with the decompositions at neighbouring instants. The obtained set of decompositions allows then to observe the time evolution of different spatial scales of the flow. This decomposition can be useful to describe non-stationary or intermittent phenomena, occurring at limited time intervals and at particular spatial scales.

Some examples of such kinds of observations are provided in Fig. 9 over shorter time intervals in order to focus on several kinds of patterns. Figure 9a (IMF 2) is an example of an eddy splitting at $t \simeq 521$ ms into a quick and a slow structures. The slower structure merges later on (at $t \simeq 523$ ms) with another structure. A similar phenomenon (merging of two eddies at $t \simeq 493$ ms) is presented in Fig. 9b, but at a higher spatial scale (IMF 3). These phenomena are not clearly observable on the original pressure data (prior to decomposition, see Fig. 6), which highlights the interest of the proposed approach.

Another type of pattern is observed in Fig. 9c. This allows to zoom on the nearly horizontal streaks observed in Fig. 8 for the IMF 5 (also present for the residue) for the

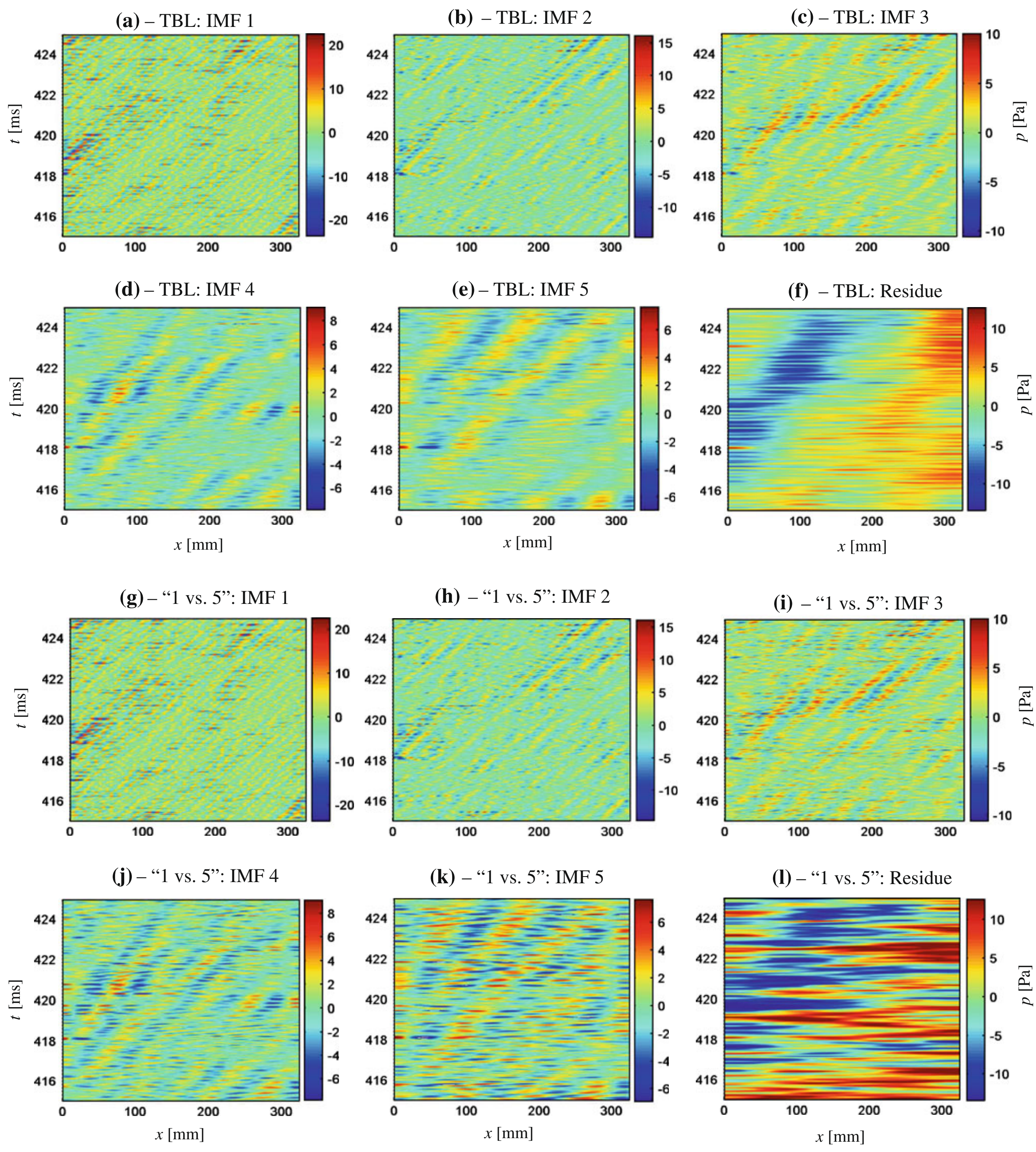

Fig. 8 Space–time representations of the five IMF and residue of the wall-pressure fluctuations under a 40 m s^{-1} turbulent boundary layer **a–f** and of the "1 versus 5" combination of TBL and diffuse sound field **g–l** after spatial E-EMD. From **a–f** and **g–l**, IMF 1–5 and residue

TBL data. These streaks are the result of aliased energy as mentioned above. The approximate frequency of these fluctuations ranges around 5 kHz, which is in the frequency range where the aliased convected energy lies in the acoustic cone (see Fig. 7 and former comments). The slopes of these fluctuations correspond roughly to a phase velocity of about ±400 m s^{-1}, that could be interpreted as an acoustic phenomena. Aliased energy can then generate, in the (x, t) plane, ambiguous fluctuations; however an investigation of the wavenumber–frequency representation (Fig. 7) permits to discard the hypothesis of acoustic fluctuations.

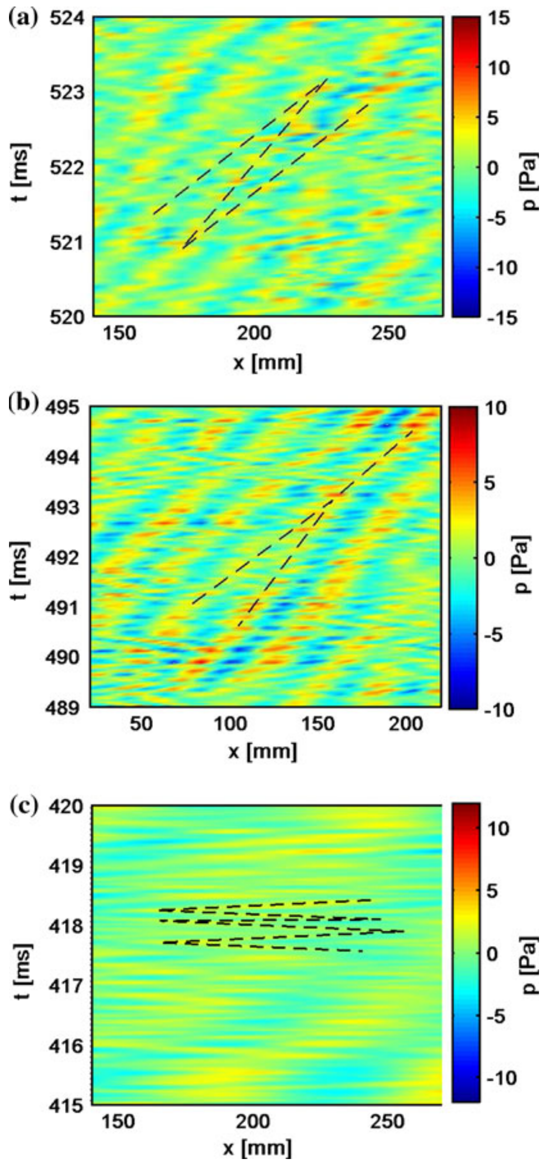

Fig. 9 Examples of observations over short time-intervals at different spatial scales; Merging and/or splitting phenomena for IMF 2 (**a**), IMF 3 (**b**), and nearly horizontal streaks for IMF 5 (**c**)

As mentioned in the Sect. 1, the original goal of this work is to develop a decomposition procedure that could separate hydrodynamic (convective) from acoustic fluctuations. For this reason, in the next section, some acoustic fluctuations are artificially combined to TBL fluctuations, in order to evaluate the potentiality of the method for hydrodynamic/acoustic separation.

4.2 Analysis of a combination of the TBL-wall-pressure fluctuations and the acoustic diffuse-sound-field pressure fluctuations

The pressure-field data of an airborne diffuse sound field, measured as explained in Sect. 2.4, are now combined to the TBL wall-pressure data. The characterization of the space–time structure of the flow-induced wall-pressure field at low (sub-convective) and very low (acoustic) wavenumbers is the object of ongoing research (e.g., numerical studies such by Hu et al. 2002; Bogey and Bailly 2008). No clear experimental evidence has been produced yet in the literature concerning the wall-pressure wavenumber frequency spectrum in the acoustic domain. Following Howe (1998, Chap. 3), we consider that the acoustic field produced by the TBL is temporally and spatially stationary, thus being very similar to a diffuse sound field. A measured diffuse sound field is used in the present experiment, in order to approach as realistically as possible what could be the acoustic fluctuations produced by a TBL at the wall boundary.

The measured energies E_{TBL} and E_{DSF} of both TBL and diffuse sound field pressure data have been first estimated. A normalization factor, $n_E = E_{\mathrm{TBL}}/E_{\mathrm{DSF}}$, is used to set the energy of the diffuse sound field time pressure signal, relatively to the TBL time pressure signal. A factor f_E is used to choose the contribution of each data set in the mixed signal. The authors studied mixed signals with f_E ranging from 1/1 to 1/500 (not presented). $f_E = 1/5$ (equivalent to 7 dB) is chosen here, as it is a good compromise between a non trivial separation task for E-EMD and a visually observable acoustic signature in the combined signal of Fig. 10. Thus, the signal combining the TBL data ($p_{\mathrm{TBL}}(x, t)$) and the diffuse sound field data ($p_{\mathrm{DSF}}(x, t)$) is obtained according to:

$$p(x,t) = p_{\mathrm{TBL}}(x,t) + n_E.f_E.p_{\mathrm{DSF}}(x,t). \tag{6}$$

In the following, this signal is referred to as the "1 versus 5" combination signal. Spatial correlogram and E-EMD techniques are then applied to this set of pressure data.

4.2.1 *The space–time and wavenumber–frequency representations of the initial combined pressure signal*

Figure 10 shows the space–time representation of the combined pressure signal. The same axes and scales as in

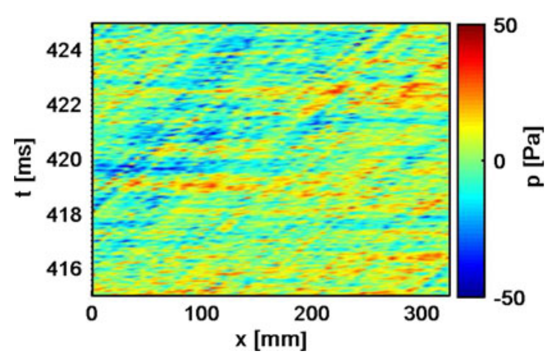

Fig. 10 Space–time representation of the "1 versus 5" combination of TBL and diffuse sound field

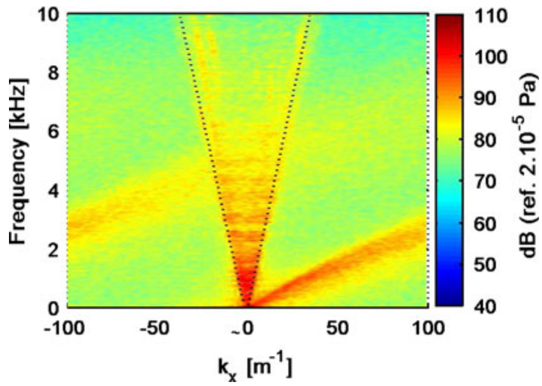

Fig. 11 Wavenumber–frequency representation of the "1 versus 5" combined data

Fig. 6 are used and, to make comparison easier, time intervals are identical.

The same set of oblique patterns as previously discussed is observed, corresponding to the convected hydrodynamic fluctuations. A new set of nearly horizontal signatures is now observed. As an almost horizontal slope indicates a very large phase velocity, these patterns are likely to be the signature of the diffuse sound field pressure fluctuations. By using a time-magnified (x, t) representation (not presented here), phase velocities ranging in the intervals $]-\infty;$ $-340]$ and $[340; +\infty[$ can be estimated. This confirms the acoustic nature of these signatures.

The application of the Spatial Correlogram method confirms the presence of both components. Figure 11 shows the wavenumber–frequency representation of the mixed pressure signal, with the same axes and scales than in Fig. 7. The convective cone is observed and, as previously explained in Sect. 4.1, the velocity is estimated to be about 32 m s^{-1}. The acoustic cone is now entirely filled by the energy brought by the acoustic pressure data; the measured diffuse sound field data introduced in the analysed signal corresponds to our expectations of classical diffuse sound fields.

4.2.2 E-EMD results of the mixed pressure signal

Figure 8g–l show the space–time representations of the five IMF and residue of the decomposition of the combined pressure signal. The axes and scales are identical to those of Fig. 8a–f (TBL pressure signal). Moreover, the color bar (in Pa) is the same for each mode (the color bar of the two IMF 1 is the same for TBL and diffuse sound field data, etc.), but are different from one mode to another, as previously explained in Sect. 4.1.

Figure 12 presents the six wavenumber–frequency representations of the five IMF and residue. The axes and scales are identical to those of Figs. 7 and 11. The spatial characteristics of the decomposition are clearly shown by these representations: each mode contains a well-delimited interval of wavenumber. The wavenumber content of each mode does not overlap (at least statistically), which proves the absence of mode mixing. In the case of wide-band hydrodynamic and acoustic data, the E-EMD then behaves like a wavenumber filter: when the order of the IMF increases, the corresponding wavenumber intervals get

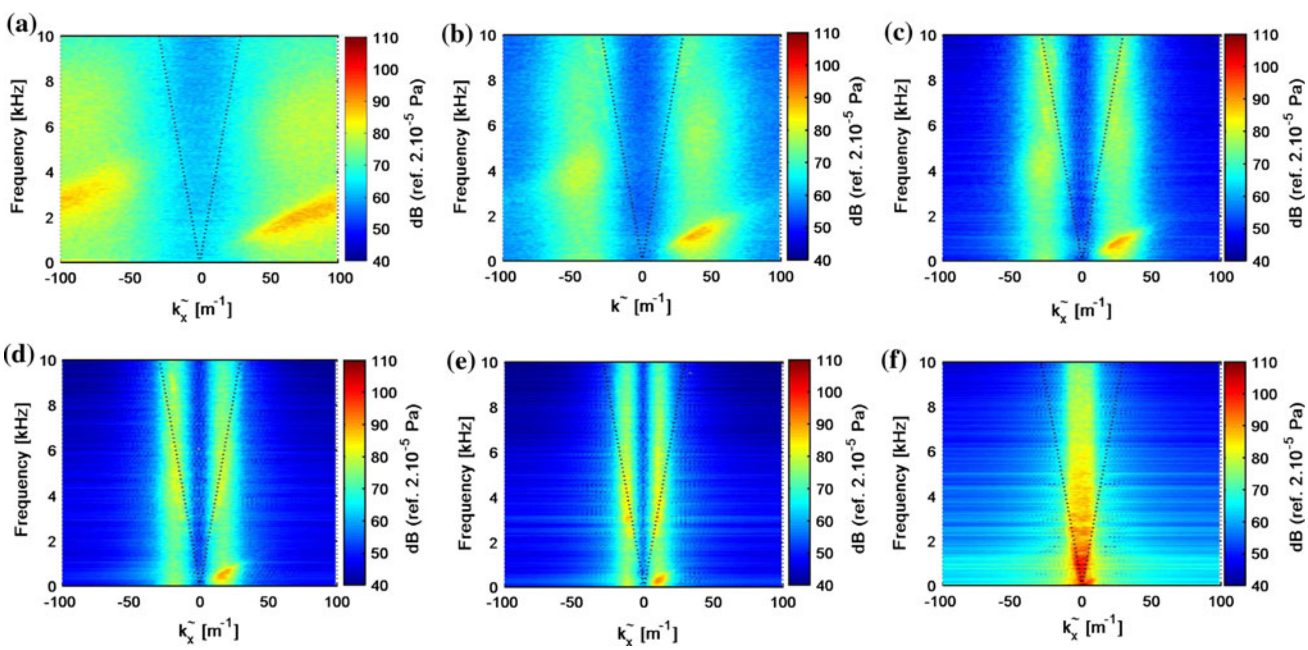

Fig. 12 Wavenumber–frequency representations of the obtained E-EMD modes for the the "1 versus 5" combined data. From **a–f**, IMF 1–5 and residue

narrower and are centred on smaller wavenumbers. Smaller spatial scales (i.e. higher wavenumbers) are then captured by lower-order IMF, and higher spatial scales are tracked by higher-order IMF. We then expect acoustic fluctuations, corresponding to higher wavenumbers than hydrodynamic fluctuations, to be contained in the high-order IMF and the residue. Flandrin et al. (2004) pointed out that for Gaussian noise signals, the EMD technique acts as a band-filter. The EMD sifting process being applied in the spatial dimension, it is then expected that this technique filters out data in the spatial dimension, i.e. according to its spatial frequencies or scales.

The two first IMF of TBL and combined data (respectively, Fig. 8a–b, g–h) exhibit almost no difference. As expected from the above considerations, the acoustic energy introduced by the diffuse sound field pressure data is not present in these IMF: only the TBL pressure fluctuations remain. This is confirmed by the observation of the wavenumber–frequency representations of these two IMF (Fig. 12): in each wavenumber interval no (or almost no) acoustic energy appears within the acoustic cone while the convective signature and its aliased artefact are clearly observed.

Gradually, as the IMF order increases, some differences appear: the set of horizontal patterns (acoustic signatures) is more and more visible. In the residue, mainly acoustic energy is present. Similarly, the wavenumber–frequency spectra (Fig. 12) shows an increasing proportion of acoustic energy in the pressure signal.

A conclusion to these last results is that the E-EMD is an efficient tool for observing flow and acoustic events at different spatial scales: indeed, it acts as a wavenumber filter. Low-order IMF capture the small-scale hydrodynamic fluctuations, as the residue and IMF with higher order mainly capture the large-scale acoustic fluctuations, plus an amount of fluctuations due to aliasing of convection phenomena. These last fluctuations could be removed by designing an array with a better spatial resolution; the aliased energy would then be rejected at higher frequencies, beyond the frequency range of interest.

5 Conclusion

This paper has investigated the possibility of using a recently developed decomposition technique, the E-EMD to analyse experimental space-time data in flows. In particular, the present application concerns wall-pressure data measured by using a linear array of 64 microphones. The E-EMD technique is used in the spatial domain: it then performs a decomposition of the wall-pressure signal, according to the spatial scales of the wall-pressure field along the array. This decomposition is carried out for each discrete instant of the dataset: it is then referred to as an "instantaneous" decomposition. The decomposition leads to six different space-time pressure fields (five IMF, and a residue function); their sum reconstructs the originally measured space-time wall-pressure field. Due to the nature of the E-EMD sifting process carried out in the algorithm, the low-order IMF collect the wall-pressure variations at smaller scales, while the high-order IMF collect the higher-scale variations.

Some applications results are provided. A first set of data considers the wall-pressure field measured under a fully developed turbulent boundary layer (TBL) in an anechoic wind-tunnel facility. The E-EMD technique is shown to be an efficient tool for enhancing non-stationary hydrodynamic phenomena occurring at some limited intervals of space and time: for instance, examples of the observation of merging and/or splitting phenomena are provided. These phenomena can be highlighted at some ranges of spatial scales by considering some particular IMF, while they do not appear on the original space-time data. However, the acoustic energy produced by the TBL, which should be a diffuse sound field, is not detected in the data.

Acoustical space-time data measured in a reverberation room, are then artificially combined to the TBL data in order to simulate a TBL wall-pressure field containing turbulence-induced noise. The acoustic energy is set 7 dB below the hydrodynamic energy. As expected, low-order IMF exhibit mainly convected pressure variations, as high-order IMF and the residue show an increasing amount of acoustic pressure perturbations. By analysing the wavenumber frequency spectra of the IMF, it can be concluded that the E-EMD technique acts approximately as a wavenumber band filter, and the wavenumber bandwidth selected by each IMF increases when the IMF order decreases. High-order IMF can then capture mainly propagative (acoustic) phenomena, as these are characterized by a low-wavenumber content, as high-wavenumber (hydrodynamic) perturbations are tracked by low-order IMF. In the context of aeroacoustical experimental studies, the proposed analysis method is then a good candidate for performing the separation of hydrodynamic and acoustic phenomena that are potentially present in experimental data.

Therefore the interests of the E-EMD technique are the following. First, it does not use a Fourier Transform, at any stage, in the time or space domain, so that it is able to perform efficient spatial filtering with a limited number of spatial samples (64 in the present study). Second, this decomposition is considered as "instantaneous", in the sense that it is performed for each discrete instant. It does not make at any point the hypothesis of temporal or spatial stationarity, unlike any other Fourier-transform-based methods. It is then possible to follow, as a function of time, the phenomena of interest in a flow, for a given interval of spatial scales (i.e., a given wavenumber interval).

Applications focusing on spatial and temporal non-stationary phenomena (such as the merging/splitting phenomena highlighted in the paper) are then in the scope of the method. This is a key-feature of the E-EMD method proposed here, opening the possibility of analysing any type of wall-pressure fluctuations (including numerical simulation results) without any a priori hypothesis on the observed phenomenon. A potential application could be, for example, the analysis of highly non-stationary large flow structures producing sound: the application of the E-EMD technique could make possible the analysis of flow events at low-order IMF, and of their instantaneous relation with the involved propagated sound perturbations, present in high-order IMF.

Acknowledgments The authors warmly acknowledge Yves Corvez, Laurent Philippon and Pascal Biais for their technical support.

References

Acarlar M, Smith C (1987) A study of hairpin vortices in a laminar boundary layer. part 2. hairpin vortices generated by fluid injection. J Fluid Mech 175:43

Ai S, Li H (2008) Gear fault detection based on ensemble empirical mode decomposition and Hilbert–Huang transform. In: Proceedings of the 2008 fifth international conference on fuzzy systems and knowledge discovery, vol 3, p 173

Arguillat B, Ricot D, Robert G, Bailly C (2005) Measurements of the wavenumber–frequency spectrum of wall pressure fluctuations under turbulent flows. In: Proceedings of 11th AIAA/CEAS aeroacoustics conference (26th AIAA aeroacoustics conference), Monterey, California

Bogey C, Bailly C (2008) Recent developments in Direct Noise Computation of turbulent flows: numerical methods and applications. In: Proceedings of 37th inter- noise congress, Shanghai, China

Corcos GM (1963) Resolution of pressure in turbulence. J Acoust Soc Am 35(2):192

Debert S, Pachebat M, Valeau V, Gervais Y (2007) Experimental wave number separation of wall-pressure fluctuations beneath a turbulent boundary layer. In: Proceedings of 19th international congress of acoustics ICA2007, Madrid

Flandrin P, Rilling G, Goncalves P (2004) Empirical Mode Decomposition as a filter bank. IEEE Sig Proc Lett 11(2):112

Fulton M, Soraghan PJJ (2006) Ensemble Empirical Mode Decomposition applied to musical tempo estimation. In: Digital music research conference DMRN-06, Goldsmiths College, University of London

Garello R (2008) Two-dimensional signal analysis. ISTE, London

Hinze JO (1975) Turbulence: an introduction to its mechanism and theory, 2nd edn. McGraw-Hill Book Co., New York

Howe MS (1998) Acoustic of fluid-structure interactions. Cambridge University Press, Cambridge

Hu ZW, Morfey CL, Sandham ND (2002) Aeroacoustics of wall-bounded turbulent flows. AIAA J 40(3):465

Huang NE, Shen SSP (2005) Hilbert–Huang transform and its applications. Interdisciplinary mathematical sciences, vol 5, World Scientific Publishing Co. Pte. Ltd, Hackensack

Huang NE, Shen Z, Long SR, Wu MC, Shih HH, Zheng Q, Yen NC, Tung CC, Liu HH (1998) The Empirical Mode Decomposition and the Hilbert spectrum for nonlinear and non-stationary time series analysis. Proc R Soc Lond A 454:953

Huang XY, Schmitt FG, Lu ZM, Liu YL (2008) An amplitude-frequency study of turbulent scaling intermittency using Empirical Mode Decomposition and Hilbert spectral analysis. Europhys Lett 84(4)

Lee I, Sung HJ (2001) Characteristics of wall-pressure fluctuations in separated and reattaching flows over a backward-facing step; part I. Time-mean statistics and cross-spectral analyses. Exp Fluids 30:262

Lei Y, He Z, Zi Y (2009) Application of the EEMD method to rotor fault diagnosis of rotating machinery. Mech Syst Signal Process 23(4):1327

Lueptow RM (1995) Transducer resolution and the turbulent wall pressure spectrum. J Acoust Soc Am 97(1):370

Panton RL, Robert G (1994) The wavenumber-phase velocity representation for the turbulent wall-pressure spectrum. J Fluids Eng 116:447

Schlichting H (1979) Boundary–Layer theory, 7th edn. McGraw-Hill, New-York

Suh J, Frankel SH, Mongeau L, Plesniak MW (2006) Compressible large eddy simulations of wall-bounded turbulent flows using a semi-implicit numerical scheme for low mach number aeroacoustics. J Comput Phys 215(2):526

Wu ZH, Huang NE (2009) Ensemble Empirical Mode Decomposition: a noise-assisted data analysis method. Adv Adapt Data Anal 1:1

Zhou X, Zhao H, Jiang T (2009) Adaptive analysis of optical fringe patterns using Ensemble Empirical Mode Decomposition algorithm. Optics Lett 34(13):2033